

# Mechanochemical Degradation of Ethylene–Propylene Copolymers: Characterization of Olefin Chain Ends

Andrew C. Kolbert,\* Joseph G. Didier, and Lisheng Xu

Analytical Research and Development, DSM Copolymer Inc., P.O. Box 2591, Baton Rouge, Louisiana 70821

Received July 25, 1996; Revised Manuscript Received October 10, 1996<sup>®</sup>

**ABSTRACT:** We have examined chain ends in ethylene–propylene (EP) copolymers following high-temperature shearing in an extruder. New chemical structures, not present prior to shearing, corresponding to vinyl, vinylidene, and vinylene chain ends were observed via  $^1\text{H}$  and  $^{13}\text{C}$  NMR and FTIR spectroscopy. A compilation of the various types of olefin chain ends possible via main chain scission of EP was made and their  $^{13}\text{C}$  chemical shifts were calculated and compared with experimental results. This comparison, in combination with the results of DEPT experiments, allowed the assignment of the olefin region of the  $^{13}\text{C}$  spectrum. The mechanism of polymer shearing appears to be hydrogen abstraction followed by disproportionation via  $\beta$ -scission of the main chain radicals to form olefins. A strong preference was shown for abstraction of methine protons, presumably due to the stability of the tertiary radical intermediate, and main chain scission at the position  $\beta$  to a methyl group.

## Introduction

The degradation of polymers by mechanical actions such as mixing and high temperature extrusion is a long established technology within the rubber and plastics industry. A great deal of attention has been given of late to the subject of “controlled rheology”,<sup>1–8</sup> in which the rheology of a polymer has been intentionally affected by either mechanical means or irradiation<sup>9,10</sup> for the purpose of improving flow characteristics, raising or lowering viscosity, and narrowing molecular weight distributions. Despite the wide use of mechanical processing technology, much of the past research has been phenomenological in nature, as it had been thought that mechanical processing led only to changes in the *bulk* properties of the material. Consequently, most work has been focused on measurements such as tensile strength, Mooney viscosity, stress relaxation, and melt-flow index which give limited insight into the micromolecular chemistry of the process.

In the past two decades a great deal of attention has been paid to the emerging field of *mechanochemistry* in which *chemical* phenomena such as cross-linking, chain scission, peroxy-radical formation, and other free radical chemical reactions are initiated by mechanical action.<sup>11–13</sup> Much of the early efforts have focused on the use of electron spin resonance (ESR) to directly observe the free radicals formed by ball-milling,<sup>14,15</sup> drilling,<sup>16</sup> slicing,<sup>17</sup> stretching,<sup>18–20</sup> sawing,<sup>21</sup> ultrasonic irradiation,<sup>22</sup> or high-speed stirring.<sup>23</sup> Recently, Sohma observed the mechano-radicals created during high-temperature extrusion by ESR combined with a spin trapping technique.<sup>24</sup> Infrared spectroscopy has been used to detect the formation of olefin groups and carbonyl groups (indicating oxidation) following the shear degradation of polyethylene.<sup>8,25,26</sup>

Nuclear magnetic resonance (NMR) spectroscopy has not been used in these applications, presumably due to its relative insensitivity as compared to other methods. This is unfortunate, as NMR is a very specific probe of the local environment, often capable of distinguishing between two carbons in structural fragments that differ

in structure four bonds away from the site of interest. It is uniquely suited to the problems of polymer degradation where chain ends are created which are fully resolved from the main chain carbons in the  $^{13}\text{C}$  NMR spectrum. The disadvantage of NMR lies in the fact that given its relative insensitivity, it is problematic acquiring a  $^{13}\text{C}$  NMR spectrum of chain ends, which comprise a small fraction of the sample.

NMR, however, has an excellent track record of providing important information about the structure and polymerization mechanisms for low molecular weight (LMW) polymers, which have a relatively high fraction of chain ends. Zambelli *et al.* have studied the stereochemistry of stereospecifically  $^{13}\text{C}$  labeled chain ends in LMW isotactic polypropylene.<sup>27,28</sup> The microstructure of LMW ethylene–1-butene copolymers has been probed via  $^1\text{H}$  and  $^{13}\text{C}$  NMR of chain ends by Rossi *et al.*<sup>29</sup> Cheng has studied the complete sequence distribution including regio- and stereoregularity effects in LMW polypropylene<sup>30</sup> and Cheng and Smith have performed a complete characterization of saturated chain ends in LMW ethylene–propylene copolymers by  $^{13}\text{C}$  NMR.<sup>31</sup>

In this paper we examine the chain ends formed in ethylene–propylene (EP) copolymers during high-temperature shearing in an extruder. The polymers were sheared from an initial number average molecular weight,  $M_n$ , of over 90 000 to less than 7000 in order to generate enough chain ends for detection with  $^{13}\text{C}$  NMR. New chemical structures, which are not present prior to shearing, corresponding to vinyl, vinylidene, and vinylene chain ends were observed via  $^1\text{H}$  and  $^{13}\text{C}$  NMR and FTIR spectroscopy. We have compiled an exhaustive list of the possible olefin chain ends produced via main chain scission of EP and calculated their  $^{13}\text{C}$  chemical shifts. A comparison of the experimentally observed shifts to the calculations, in addition to the results of DEPT experiments, allowed the complete assignment of the olefin region of the  $^{13}\text{C}$  NMR spectra of the sheared samples. The implications of the relative concentrations of chain ends for the mechanism of polymer shearing will be discussed.

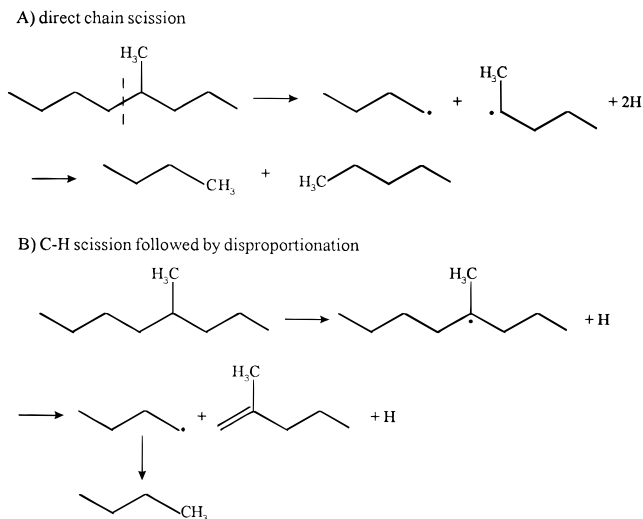
## Background

**Mechanisms.** High-temperature extrusion of polymers for viscosity reduction is a common practice in the

\* Corresponding author.

<sup>®</sup> Abstract published in *Advance ACS Abstracts*, December 1, 1996.

Scheme 1



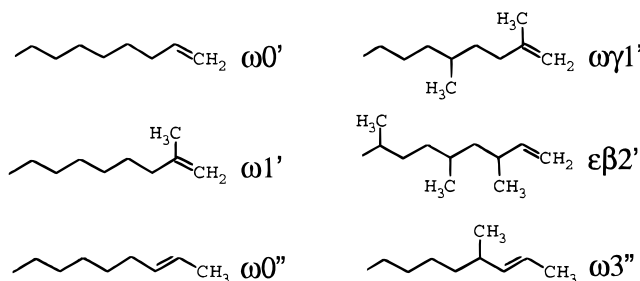
rubber and plastics industry. On a molecular level, this process accomplishes three things. First, it reduces the average molecular weight by reducing the average polymer chain length. Second, it narrows the molecular weight distribution, as shearing forces preferentially cleave polymer chains near the center.<sup>32</sup> Lastly, it generates scission induced radicals, which can then undergo a variety of chemical reactions. There have been two proposed models for chain scission in polyolefins, as illustrated in Scheme 1.

Direct chain scission, Scheme 1A, generally leads to saturated chain ends and has been reported as the preferred route for degradation of ethylene-propylene copolymers under  $\gamma$ -irradiation.<sup>10</sup> Hydrogen abstraction followed by disproportionation leads to the formation of olefins, as illustrated in Scheme 1B. Direct chain scission can also lead to olefins via a recombination reaction (not shown) in which the primary radical abstracts a  $^1\text{H}$   $\alpha$  to the secondary radical, forming a saturated chain end and a vinyl or vinylene chain end. This mechanism requires the existence of a free radical sphere of activity or "cage" in which the radicals reside, following chain scission.<sup>8</sup> It has been postulated, however, that under conditions of high mechanical shear, these cages are destroyed, discriminating against the recombination reaction.<sup>8</sup>

The radical intermediates formed in either mechanism can participate in a molecular enlargement reaction, involving the formation of long chain branches, as Rideal and Padgett have observed in high-density polyethylene (HDPE).<sup>8</sup> At lower shearing temperatures ( $<290^\circ\text{C}$ ), the number average molecular weight,  $M_n$ , and molecular weight distribution (MWD) from size exclusion chromatography (SEC) were observed to increase, while at temperatures above  $290^\circ\text{C}$ , both  $M_n$  and MWD were reduced.<sup>8</sup> All of the samples discussed in this paper were sheared at temperatures ranging from  $360$  to  $400^\circ\text{C}$ , and both a reduction in  $M_n$  and a narrowing of the MWD were observed.

Olefin structures have been previously observed in ethylene-propylene copolymers. The chain termination of ethylene-propylene copolymerization using Ziegler-Natta catalysts has been proposed to be a  $\beta$ -hydride transfer to the monomer, in the absence of chain transfer agents, on the basis of the identification of vinyl, *trans*-vinylene, and vinylidene end groups by IR.<sup>33</sup> Cheng and Smith<sup>31</sup> and Tsutsui *et al.*<sup>34</sup> have observed vinylidene groups only, in the  $^{13}\text{C}$  NMR spectrum of

Chart 1



LMW EP, which vanished when hydrogen was present in the reactor during polymerization.<sup>31</sup> As hydrogen was used in the polymerization of the samples discussed below, no terminal unsaturation existed prior to sample shearing.

**Nomenclature.** In order to discuss the large variety of possible unsaturated chain ends, it is necessary to define some notation. We propose an extension of the notation of Cheng and Smith,<sup>31</sup> originally designed for saturated chain ends. To review, each chain end is designated by a three-character code. The rightmost character is a number representing the distance from the first methyl substituent to the chain end. The first Greek letter to the left represents the distance from the first methyl substituent from the chain end to the second methyl substituent, and the leftmost character represents the distance of the first methyl substituent to the third one. If no such third methyl group exists or if its presence is irrelevant, this is designated by the letter  $\omega$ . For simplicity, the unsubstituted straight chain is designated  $\omega 0$ .

For the case of unsaturated chain ends, we propose the addition of a ' or '' to represent the position of the double bond, originating at either the C1 position, the chain end, or the C2 position, one carbon from the end. For example, the three main structural families vinyl, vinylidene, and vinylene, illustrated in Chart 1, are designated  $\omega 0'$ ,  $\omega 1'$ , and  $\omega 0''$ , respectively. Examples for other structures follow.

**Unsaturated Chain End Structures and Predicted  $^{13}\text{C}$  Chemical Shifts.** There are 29 possible saturated structures generated by random placements of ethylene and propylene near the chain end.<sup>31</sup> Unsaturation adds an additional level of complexity, as we have, in addition to those skeleton structures, the position of the double bond to consider. This may be either C1-C2 which generates the vinyl and vinylidene structural families, or C2-C3 which generates the vinylene structures. Lastly, we must consider the stereochemistry across the C2-C3 double bond. We now have 77 different structures, which are compiled in Table 1. Many of these structures are spectroscopically degenerate, resulting in 32 distinguishable structural families.

The calculation of chemical shifts was performed on all 77 structures, and they were grouped into the families subsequently. In many cases an experimental spectrum existed for a model compound which approximates a fragment of interest. Wherever possible we have used experimental shifts from model compounds rather than calculation. Where calculation was required, we used a database containing an experimental spectrum from a model compound as closely related as possible to the fragment under consideration. The reference column reports the model olefin used, where appropriate. Error estimates on the shifts overall are

Table 1. Olefin Chain Ends and Their Chemical Shifts<sup>a</sup>

no.	code	structure	<sup>13</sup> C chemical shifts (ppm)			ref	present?
			C3	C2	C1		
1	$\omega 0'$	...0000000		139.1	114.2	35	+
2	$\omega 1', \omega \delta 1', \omega \epsilon 1'$	...00000 <u>10</u>		145.8	110.3	31	+
				146.1	109.8	36	
3	$\omega 2', \omega \gamma 2', \omega \delta 2', \omega \epsilon 2', \epsilon \gamma 2'$	...0000100		145.1	112.3	35	+
4	$\omega 3', \omega \beta 3', \omega \gamma 3', \omega \delta 3', \delta \beta 3'$	...0001000		137.8	115.4	37	+
5	$\omega 4', \omega \beta 4', \omega \gamma 4', \omega \delta 4', \delta \beta 4'$	...0010000		139.3	114.1	38	+
6	$\omega 5'$	...0100000		137.1	114.1	39	+
7	$\omega 6'$	...1000000		138.5	113.6	39	+
8	$\omega \beta 1', \delta \beta 1', \epsilon \beta 1'$	...00010 <u>10</u>		144.6	111.8	31	+
				144.8	111.3	40	
9	$\omega \beta 2', \delta \beta 2', \epsilon \beta 2'$	...0010100		144.8	112.3	39	+
10	$\omega \gamma 1', \epsilon \gamma 1'$	...00100 <u>10</u>		146.2	110.3	39	+
11	$\omega 0'' (E)$	...0000000	131.8	124.6	17.9	35	+
			132.1	124.7	18.0	41	
12	$\omega 0'' (Z)$	...0000000	131.2	123.8	12.8	41	—
13	$\omega 1'', \omega \epsilon 1''$	...00000 <u>10</u>	125.2	131.1	17.6	42	+
					25.7		
14	$\omega 2'', \omega \delta 2'', \omega \epsilon 2'' (E)$	...0000100	135.9	118.4	13.3	43	—
15	$\omega 2'', \omega \delta 2'', \omega \epsilon 2'' (Z)$	...0000100	136.1	119.2	13.3	43	—
16	$\omega 3'', \omega \gamma 3'', \omega \delta 3'' (E)$	...0001000	137.6	123.0	18.0	44	—
17	$\omega 3'', \omega \gamma 3'', \omega \delta 3'' (Z)$	...0001000	137.3	122.4	13.0	44	—
18	$\omega 4'', \omega \beta 4'', \omega \gamma 4'', \omega \delta 4'', \delta \beta 4'' (E)$	...0010000	130.4	125.8	17.9	45	—
19	$\omega 4'', \omega \beta 4'', \omega \gamma 4'', \omega \delta 4'', \delta \beta 4'' (Z)$	...0010000	129.7	124.4	12.8	45	—
20	$\omega 5'' (E)$	...0100000	132.5	124.7	17.7	39	+
21	$\omega 5'' (Z)$	...0100000	131.7	123.8	12.8	39	—
22	$\omega 6'' (E)$	...1000000	132.1	124.7	17.5	39	+
23	$\omega 6'' (Z)$	...1000000	131.2	123.8	12.3	39	—
24	$\omega \beta 1'', \epsilon \beta 1''$	...00010 <u>10</u>	133.0	128.9	25.7	46	+
					17.7		
25	$\omega \beta 2'', \delta \beta 2'', \epsilon \beta 2'' (E)$	...0010100	135.5	118.8	9.3	39	—
26	$\omega \beta 2'', \delta \beta 2'', \epsilon \beta 2'' (Z)$	...0010100	135.7	119.5	9.3	39	—
27	$\omega \beta 3'', \delta \beta 3'' (E)$	...0101000	138.0	123.0	19.2	39	—
28	$\omega \beta 3'', \delta \beta 3'' (Z)$	...0101000	137.7	122.5	7.8	39	—
29	$\omega \gamma 1'', \epsilon \gamma 1''$	...00100 <u>10</u>	123.9	131.7	25.8	47	+
					17.8		
30	$\omega \gamma 2'', \epsilon \gamma 2''$	...0100100	139.5	118.8	15.8	39	—
31	$\omega \delta 1''$	...10000 <u>10</u>	125.3	130.8	25.7	48	+
					17.6		
32	$\delta \beta 1''$	...0101010	129.7	129.8	25.7	39	—
					17.6		

<sup>a</sup> A 1 in the structure column represents a methyl group attached to a methine carbon, while a 0 represents a methylene. The two carbons connected by the double bond are underlined. The carbons are numbered from the chain end. A "+" in the "present?" column indicates that resonances which may indicate the presence of this structure are observed in the <sup>13</sup>C spectra of Figure 4.

approximately  $\pm 0.5$  ppm, with somewhat higher estimates for the calculated shifts, perhaps  $\pm 1$  ppm.

## Experimental Section

EP68 is an ethylene-propylene copolymer, with an average ethylene content of approximately 68 mol % made with a Ziegler-Natta-type vanadium-based catalyst. Hydrogen was present in the reactor and was used for molecular weight control. The unsheared EP68 contained 0.4 wt % 5-vinyl-2-norbornene as a third monomer, as measured by FTIR. Sheared EP68 samples were prepared with a single pass through a twin screw extruder (Werner and Pfleiderer ZSK-30, Ramsey, NJ), the differences between samples being limited to the set point in the high-temperature, high-shear region of the extruder. The extrusions were performed under a nitrogen blanket to prevent the sheared polymer from being contaminated with ketones.<sup>24</sup> No carbonyl band was observed in the FTIR spectra of the sheared polymers immediately after shearing.

NMR spectra were acquired on a Bruker AC-300 pulsed NMR spectrometer (Bruker Instruments, Billerica, MA) equipped with a 7.4 T superconducting magnet operating at <sup>1</sup>H and <sup>13</sup>C frequencies of 300 and 75 MHz, respectively. Experimental temperatures were 125 °C, and all spectra were referenced to TMS, using HMDS as an internal standard. <sup>1</sup>H spectra were acquired as 10% solutions in *o*-dichlorobenzene-*d*<sub>4</sub> (ODCB-*d*<sub>4</sub>) (Isotec, Miamisburg, OH), typically using 64–512 scans with a minimum recycle time of 15 s. <sup>13</sup>C spectra were run as solutions in either ODCB-*d*<sub>4</sub> or tetrachloroethane-

*d*<sub>2</sub> (TCE-*d*<sub>2</sub>), with concentrations ranging from 25 to 50% in order to attain the required sensitivity. ODCB-*d*<sub>4</sub> is an excellent solvent; however, it has lines in the vinylene region of the <sup>13</sup>C spectrum. TCE-*d*<sub>2</sub> does not have lines in this region but tends to degrade the double bonds in the sample. The vinylidene groups are particularly sensitive to this degradation, as evidenced by the decrease in the 4.7 ppm vinylidene resonance in the <sup>1</sup>H NMR spectra, and the deep brown color of the samples after experiments lasting several days at 125 °C. <sup>13</sup>C NMR spectra typically required 10 000–50 000 scans to acquire acceptable signal-to-noise ratios. Quantitative spectra utilized a 20 s recycle time with inverse gated decoupling, though typical spectra were acquired with a recycle time of 6 s, a 75° pulse angle, and decoupling during both acquisition and the recycle time to take full advantage of the NOE effect.

<sup>13</sup>C NMR spectral simulations were performed with the CNMR program (Advanced Chemistry Development, Ontario, Canada), which uses a fragment database in addition to additivity rules. The calculated chemical shifts utilized a user-defined database containing the experimental chemical shifts of olefin model compounds from refs 35 and 41. The use of such a closely related database dramatically improved the quality of the calculated shifts in this paper, which we believe to be accurate to  $\pm 1$  ppm.

FTIR spectra were acquired on films spread upon KBr windows on a 20SXB Nicolet FTIR spectrometer (Nicolet Instruments, Madison, WI). FTIR spectral processing and integration were performed using the Nicolet OMNIC software

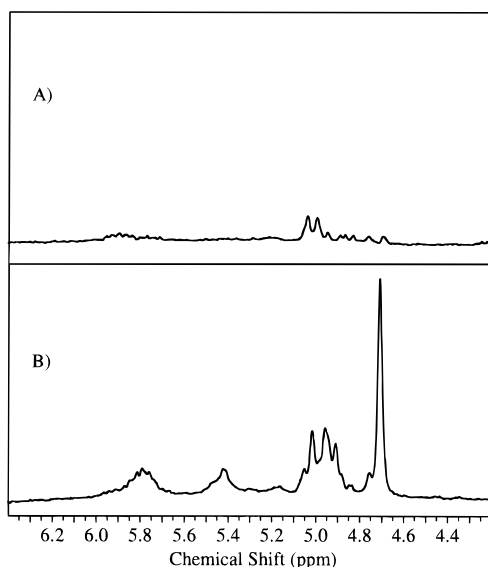


**Figure 1.** High-resolution  $^1\text{H}$  NMR spectra of EP68. The vertical scale has been expanded by a factor of 600. Both spectra have been normalized so that the aliphatic methylene resonances have equal intensity. (A) Spectrum of unsheared EP68 in  $\text{ODCB-}d_4$ . Note the vinyl resonances at 5.0 and 5.8 ppm due to the presence of 0.4 wt % VNB. (B) Spectrum of EP68 sheared at 400  $^\circ\text{C}$ . In addition to increased intensity in the vinyl regions, resonances at 4.7 and 5.4 ppm are observed, corresponding to vinylidene and vinylene groups, respectively.

package. SEC measurements were performed at 135  $^\circ\text{C}$  in 1,2,4-trichlorobenzene on a Waters 150-C size exclusion chromatograph.

## Results

Figure 1 displays the olefin region of the  $^1\text{H}$  NMR spectra of (A) EP68 and (B) EP68 after high-temperature extrusion at 400  $^\circ\text{C}$ . As EP68 has 0.4 wt % 5-vinyl-2-norbornene, we expect to see the vinyl  $^1\text{H}$ 's observed at 5.0 and 5.8 ppm. After high-temperature shearing, new resonances appear in the olefin region at 4.7 and 5.4 ppm, in addition to an increase in intensity of the lines at 5.0 and 5.8 ppm. By comparison with spectra from model compounds, we can assign the 4.7 and 5.4 ppm resonances to vinylidene and vinylene  $^1\text{H}$ 's, respectively.

These assignments can be easily confirmed by FTIR. The C–H bending modes of vinylidene, vinyl, and *trans*-vinylene are observed at 888, 909, and 965  $\text{cm}^{-1}$ , respectively.<sup>25,33,49,50</sup> Figure 2 illustrates the 820–980  $\text{cm}^{-1}$  region of the FTIR spectrum of EP68 following various degrees of shear. The uppermost trace is the spectrum from unsheared EP68, in which the vinyl group C–H bending mode may be easily seen at 909  $\text{cm}^{-1}$ . There is clearly no vinylidene band in the unsheared polymer, though there is an interference obscuring the *trans*-vinylene region. With sample shearing, the intensities of both the vinyl and vinylidene bands increase, as compared with the  $\text{CH}_{2,n}$  ( $n \geq 4$ ) “breathing band”, present at 721  $\text{cm}^{-1}$ .

The concentrations of these groups can be easily measured with  $^1\text{H}$  NMR, by calculating the integral ratio of the relevant olefin resonance to the main chain aliphatic resonance from 0.0 to 3.0 ppm, after accounting for the relative number of  $^1\text{H}$ 's on each group. These results are summarized in Table 2 for the EP68 samples prepared at different shearing temperatures, along with the number average molecular weight from size exclusion chromatography (SEC).

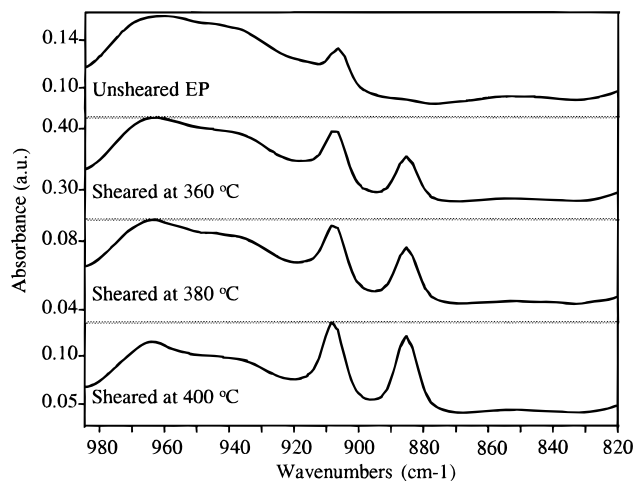


**Figure 2.** FTIR spectra of EP68 as a function of shearing temperature. Note the increase of the vinyl, vinylidene, and *trans*-vinylene C–H bending bands at 909, 888, and 965  $\text{cm}^{-1}$  respectively, with increasing shearing temperature.

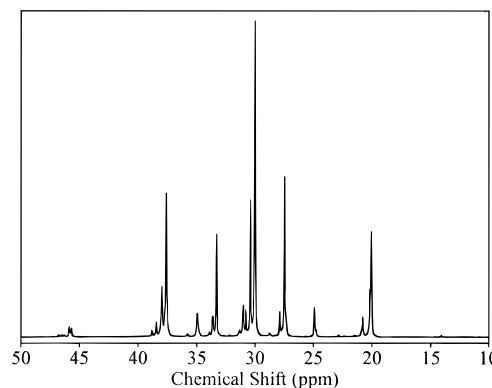


**Figure 3.**  $^{13}\text{C}$  NMR spectrum of sheared EP68 in  $\text{ODCB-}d_4$  with inverse gated decoupling. A total of 2500 scans were added with a recycle time of 20 s.

**Table 2.** Number Average Molecular Weights,  $M_n$ , from SEC, and Concentrations of Various Olefin End Groups As Measured by  $^1\text{H}$  NMR, Reported as Double Bonds per Thousand Carbons, a Unit Independent of the Chemical Identity of the Moiety

temp of shearing ( $^\circ\text{C}$ )	$10^{-3} M_n$	vinyl (C=C/1000 C)	vinylidene (C=C/1000 C)	vinylene (C=C/1000 C)	total unsaturation (C=C/1000 C)
unsheared	91.3	0.63	0	0	0.63
360	20.9	0.65	0.41	0.15	1.2
380	18.7	0.78	0.60	0.28	1.7
400	7.7	1.3	1.0	0.5	2.8

Figure 3 is a  $^{13}\text{C}$  NMR spectrum of EP68 in *o*-dichlorobenzene- $d_4$ , acquired with inverse gated decoupling under quantitative conditions. Peak assignments were made by comparison with spectra reported by Carman *et al.*<sup>51</sup> and Randall.<sup>52</sup> The ethylene content was calculated by averaging the results of the methods of Randall<sup>52</sup> and Cheng,<sup>53</sup> recently reviewed by DiMartino and Kelchtermans,<sup>54</sup> and the triad distribution was calculated according to the method of Kakugo *et al.*<sup>55</sup> These results are summarized in Table 3 for both the unsheared and 400  $^\circ\text{C}$  sheared samples.

The  $^{13}\text{C}$  NMR spectrum of EP68 sheared at 400  $^\circ\text{C}$  is displayed in Figure 4. In order to attain acceptable signal-to-noise ratios, quantitation was sacrificed by using a 6 s recycle time with composite pulse decoupling on full time to gain the maximum NOE enhancement. Figure 4A displays the olefin region from 136 to 148

**Table 3. Ethylene Sequencing via  $^{13}\text{C}$  NMR<sup>a</sup>**

	Unsheared	sheared (400 °C)
<b>Sequencing Data</b>		
mol % ethylene	68.1	68.5
$\langle N \rangle$	4.95	5.07
$E(N \geq 3)$	0.49	0.47
<b>Triad Distribution</b>		
EEE	0.34	0.35
PEE	0.29	0.29
PEP	0.06	0.07
EPE	0.17	0.18
PPE	0.11	0.10
PPP	0.02	0.02

<sup>a</sup>  $\langle N \rangle$  is the mean number of ethylenes in sequences of three and larger, and  $E(N \geq 3)$  is the fraction of ethylene in sequences of three and larger.<sup>56</sup>

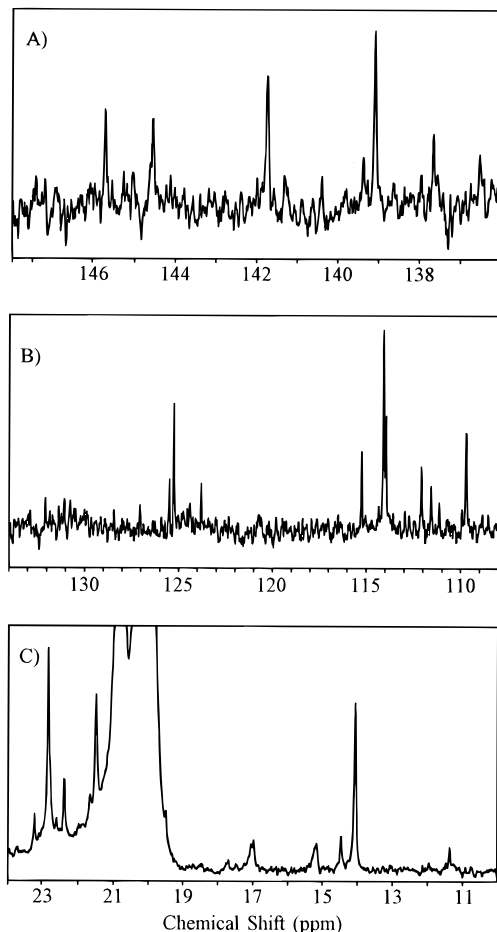


**Figure 4.** High-resolution  $^{13}\text{C}$  NMR spectra of EP68 sheared at 400 °C: (A) olefin region 136–148 ppm, solution in  $\text{ODCB-}d_4$ ; (B) olefin region 108–134 ppm, solution in  $\text{TCE-}d_2$ ; (C) aliphatic region 10–24 ppm, solution in  $\text{ODCB-}d_4$ . A total of 50 000 scans were acquired with a recycle time of 6 s and a pulse angle of 75°. Composite pulse decoupling was employed and kept on during the recycle time to take full advantage of the NOE effect. The intensities in these spectra are therefore not quantitative.

ppm of a spectrum of EP68 in  $\text{ODCB-}d_4$ . The two  $\omega 1'$  and  $\omega 1''$  vinylidene chain ends observed by Cheng and Smith<sup>31</sup> are evidenced by the C2 resonances at 145.7 and 144.6 ppm, respectively, in addition to several others. These lines are quaternary carbons and therefore are small compared to other NOE enhanced resonances, despite the relatively high vinylidene concentration. The corresponding C1 vinylidene resonances are seen at 110 and 111–112 ppm, respectively, in Figure 4B. The spectrum of Figure 4B was acquired in

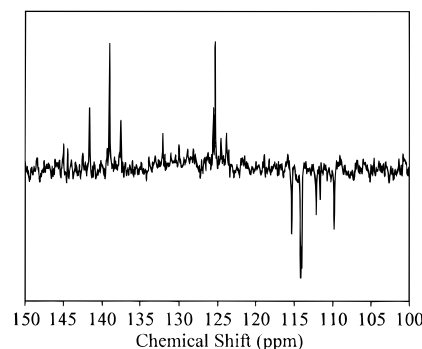


**Figure 5.**  $^{13}\text{C}$  spectrum from the DEPT-135 experiment. A total of 50 000 scans were acquired with a 6 s recycle time. The data were processed with 2 Hz exponential line-broadening.

tetrachloroethane- $d_2$  in order to avoid solvent lines in the aromatic region. C2 and C1 vinyl group resonances are seen at  $\sim 114$  and 136–140 ppm, respectively, while vinylene resonances are observed between 123–127 and 129–133 ppm. The specific assignments are summarized in Table 4. In ambiguous cases we have chosen to include structural families in which resonances appear in the appropriate locations, unless there is evidence to the contrary. Although we have listed members of the  $\delta\beta n'$  and  $\delta\beta n''$  families, the low concentration of PPP triads, as seen in Table 3, would seem to rule out any detectable concentration of these end groups.

The NMR spectrum from the DEPT-135 experiment, illustrated in Figure 5, was of great utility in assigning the olefin resonances. The DEPT-135 experiment yields a spectrum with primary and tertiary carbons phased up, secondary carbons phased down, and quaternary carbons missing. The last column of Table 4 reflects the results of the DEPT experiments. In cases in which a large number of possible chain end resonances overlap, it may be difficult to determine whether or not a quaternary carbon contribution is missing. In that case, we have chosen to include, rather than exclude, the structure.

The aliphatic region of sheared EP68 in  $\text{ODCB-}d_4$  is displayed in Figure 4C. Cheng and Smith<sup>31</sup> have performed an exhaustive analysis of this region of the spectrum for low molecular weight EP, and there are few notable differences found here. We have observed the C1  $\omega 2$  chain end at 11.3 ppm predicted, but not observed, by Cheng and Smith. This chain end was also recently observed by O'Donnell and Whittaker in  $\gamma$ -irradiated EP.<sup>10</sup> Further, some of the intensity in the 16.8–18.0 ppm region may be due to the C1 methyl groups of the *trans*-vinylene chain end families.

## Discussion

**Ethylene Sequencing Statistics.** The mole percent ethylene appears to increase with sample shearing, as reported in Table 3. FTIR measurements also show an ethylene content increase upon shearing from 68.1 to 68.9 mol %. The precision on both NMR and FTIR measurements is approximately  $\pm 1$  mol %, so these differences are not statistically significant, however it is useful to consider whether or not an observed change is physically reasonable.

The unsheared EP68 with  $M_n = 91.3\text{k}$  has an average chain length  $\langle L \rangle = 5636$ , assuming an average "link" mass of 16.2 g/mol. The polymer sheared at 400 °C, with  $M_n = 7.7\text{k}$  from SEC, has an average chain length

**Table 4.**  $^{13}\text{C}$  Chemical Shifts and Assignments of the Spectrum of Sheared EP<sup>a</sup>

shift (ppm)	mechanochemically created olefin chain ends	structure families	DEPT results
145.7	2- $\omega 1'$ , 2- $\omega\gamma^+1'$ , 2- $\epsilon\gamma 1'$	2, 10	Q
145.0–145.3	2- $\omega 2'$ , 2- $\omega\gamma^+2'$ , 2- $\epsilon\gamma 2'$	3	T
144.6	2- $\omega\beta 1'$ , 2- $\delta^+\beta 1'$ , 2- $\omega\beta 2'$ , 2- $\delta^+\beta 2'$	8, 9	Q, T
141.7	C8 (vnb)		T
138.5–139.5	2- $\omega 0'$ , 2- $\omega 6^{++}$ , 2- $\omega 4'$ , 2- $\omega\beta^+4'$ , 2- $\delta\beta 4'$	1, 5, 7	T
137.7, 136.5	2- $\omega 3'$ , 2- $\omega\beta^+3'$ , 2- $\delta\beta 3'$ , 2- $\omega 5'$	4, 6	T
127–133	3- $\omega 0''$ , 3- $\omega 5^{++}$ , 2,3- $\omega\beta^+1''$ , 3- $\epsilon\beta^+1''$ , 2- $\omega 1''$ , 2- $\omega \delta^+1''$	11, 13, 20, 22, 24, 29, 31	T, Q (?)
125.5	3- $\omega 1''$ , 3- $\omega\delta^+1''$	13, 31	T
125.3	2- $\omega 0''$ , 2- $\omega 5^{++}$	11, 20, 22	T
123.8	3- $\omega\gamma 1''$ , 3- $\epsilon\gamma 1''$	29	T
115.4	1- $\omega 3'$ , $\omega\beta^+3'$ , $\delta\beta 3'$	4	S
114.3, 114.2	1- $\omega 0'$ , 1- $\omega 4^{++}$ , $\omega\beta^+4'$ , $\delta\beta 4'$ , C-9 (vnb)	1, 5, 6, 7	S
112.3	1- $\omega 2'$ , $\omega\gamma^+2'$ , $\epsilon\gamma 2'$	3	S
111.5–111.8	1- $\omega\beta 1'$ , $\delta^+\beta 1'$	8	S
110.0	1- $\omega 1'$ , 1- $\omega\gamma^+1'$ , 1- $\epsilon\gamma 1'$	2, 10	S

<sup>a</sup> The structure families refer to Table 1. The number in front of the structure symbol designates the assigned carbon, counting from the chain end. A "+" superscript on a symbol designates that chain end and all chain ends generated by incrementing that symbol.

of  $\langle L \rangle = 475$ . For the low molecular weight of the polymer sheared at 400 °C, we can measure  $M_n$  directly from the ratio of the chain ends to the main chain resonances in the quantitative NMR spectrum, which yields  $M_n = 6420$ ,  $\langle L \rangle = 396$ . As SEC results are subject to calibration uncertainties, the  $M_n$  from NMR is believed to be more accurate.

For the original polymer chain with  $\langle L \rangle = 5636$ , we have on average 2 chain ends, while for the highly sheared polymer, the same length of chain has  $(5636/396) \times 2 = 28.5$  chain ends. If we assume from the  $^1\text{H}$  NMR results (see below) a 1.2:1 preference for scission at a propylene unit, we lose 15.5 propylene units and 13.0 ethylene units due to scission, resulting in an ethylene content of 68.2 mol %. Even assuming that scission solely occurs at PP linkages, which loses 28.5 propylenes to shearing, results in a sheared polymer ethylene content of 68.5 mol %. Clearly, the increase in ethylene content due to preferential chain scission is a minor effect, below the statistical precision of the measurement for most shearing conditions.

The other sequencing statistics can give some insight into the sort of chain ends which might appear upon polymer degradation. For instance, though 66% of the triads contain a propylene group, only 11% contain a PP diad, and only 2% a PPP triad. This distribution will render resonances from members of the  $\omega\beta n'$  and  $\omega\beta n''$  series comparatively difficult to observe, and members of the  $\delta\beta n'$  and  $\delta\beta n''$  series nearly impossible. Further, the fact that 34% of the triads are EEE sequences should make the  $\omega 0'$  lines the most prominent olefin resonances, at 114 and 139 ppm. Though this is observed, the resonances are not as intense as one might expect from the sequencing statistics alone. This is due to preferential chain cleavage and is discussed below. Note that there are no significant differences between the sequence distributions for un-sheared and sheared samples.

**Consumption of Vinyl Groups of VNB during Shearing.** The concentration of double bonds as a function of number average molecular weight is illustrated by Figure 6. The non-zero intercept at  $M_n = 91.3\text{k}$ , for the vinyl group curve, is due to the starting concentration of vinylnorbornene (VNB). Note the slow rise in the concentration of vinyl groups with lowering  $M_n$ , as compared with the vinylene and vinylidene groups. VNB is often included as a termonomer to promote branching due to its high reactivity.<sup>57</sup> This is due to the ease of abstraction of a  $^1\text{H}$  from the C8 carbon leading to the highly stable allylic radical. Conse-

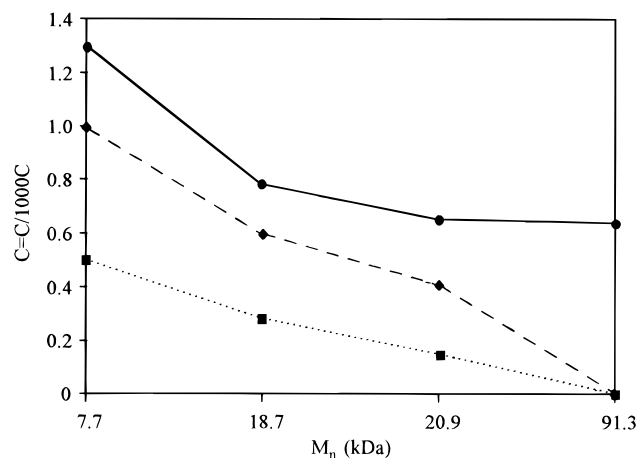
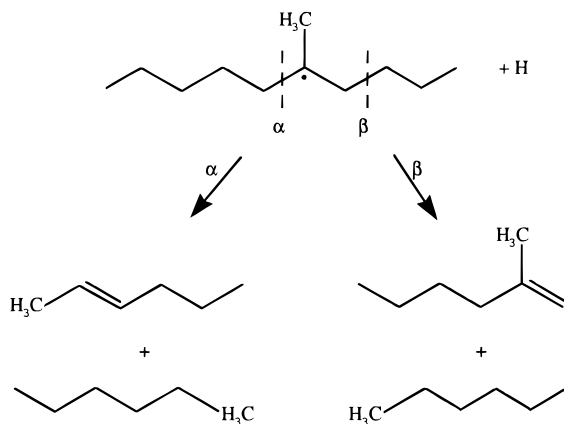


**Figure 6.** Concentrations of vinyl (solid circles, solid line), vinylidene (solid diamond, dashed line), and vinylene (solid squares, dotted line) chain ends, as measured by  $^1\text{H}$  NMR versus the number average molecular weight as measured by SEC (nonlinear scale).

quently, it should not be surprising that under conditions of high-temperature extrusion, some of the VNB vinyl groups are participating in long chain branching reactions,<sup>57</sup> the branches subsequently being sheared in a reaction which probably involves cleavage of the ring structure of the norbornene moiety. The decrease in vinyl group concentration with increasing temperature during shear degradation has been observed in HDPE with high vinyl content.<sup>8</sup> This loss of vinyl groups competes with the creation of vinyl groups by C–H scission followed by disproportionation. More support for this idea can be gathered by considering the relative changes in the concentrations of the olefin groups with changing shearing conditions.

**Mechanistic Considerations.** The evidence appears to support the mechanism of Scheme 1B. In addition to the presence of terminal unsaturation, this mechanism predicts the creation of equal numbers of saturated and unsaturated chain ends during shearing. This is confirmed through the integration of the quantitative  $^{13}\text{C}$  spectrum (not shown). Further, one olefin group is predicted to have been created for each cleaved chain. For EP68 sheared at 400 °C, if we assume an average chain length  $\langle L \rangle = 396$ , from above, for which there are two chain ends ignoring branching, we expect 5.05 chain ends per 1000 carbons, or 2.5 C=C/1000 C, in good agreement with the total unsaturation reported in Table 2 from  $^1\text{H}$  NMR. The agreement is less satisfactory for the samples sheared at 360 and 380 °C,

Scheme 2



which we predict, on the basis of the  $M_n$ 's from SEC, to have total unsaturations of 0.78 and 0.87 C=C/1000 C, respectively. There are two reasons to expect differences for these samples. First, as discussed above, the VNB unsaturation has a contribution at these lower shearing temperatures. Second, the SEC calibration uncertainties contribute to the error. The sample sheared at 400 °C is the only one which had a large enough number of chain ends to allow the measurement of  $M_n$  with  $^{13}\text{C}$  NMR.

Now let us consider the *relative* concentrations of olefin chain ends for the sheared polymers, summarized in Table 2. Following the creation of the tertiary radical and during the formation of the double bond, the chain scission can occur at position  $\alpha$  or  $\beta$  relative to the propylene group, forming the vinylene and vinylidene groups, respectively (see Scheme 2).

Vinylene groups can also be created via direct  $\alpha$ -chain scission, followed by abstraction of a secondary proton, as discussed above. The vinyl group, in contrast, is created primarily via disproportionation from a secondary radical. The ratio of the concentration of vinylidene and vinylene chain ends to that of the vinyl group chain ends will yield the ratio of tertiary to secondary radical intermediates created during shearing.

If we assume that the vinyl group concentration, due to VNB, does not change with sample shearing, we can calculate the (vinylidene + vinylene):vinyl group ratios (T:S) from Table 1, by subtracting 0.63 C=C/1000 C from the vinyl group concentration in the third column. The calculated T:S ratios are

360 °C	28:1
380 °C	5.9:1
400 °C	2.2:1

Unless we are to propose drastically different chain scission mechanisms for data separated by 20 °C, this variance is clearly absurd. If instead we calculate T:S by using the *differences* between concentrations of olefins in samples sheared at different temperatures we obtain T:S = 1.0:1 (380 °C data – 360 °C data) and T:S = 1.19:1 (400 °C data – 380 °C data). Using the 400 °C data alone, without considering VNB, gives T:S = 1.15:1. The close agreement between T:S for the 400 °C data and the 400 °C – 380 °C data indicates that most of the VNB unsaturation is consumed by shearing at 400 °C.

The relative propensity to form tertiary radicals, during mechanochemical degradation must take into account the relative concentration of secondary carbons, which can be estimated from the ethylene content plus

one-half the propylene content. With this correction the relative preference for  $^1\text{H}$  abstraction to form tertiary radicals, using T:S = 1.19:1, becomes 6.2:1.

The relative preference for  $\beta$  versus  $\alpha$  scission is simply the ratio of vinylidene to vinylene groups and is 2.3:1 averaged over the three temperatures used in this study. These results could be affected by disproportionation of secondary radicals  $\alpha$  to methyl groups, but given the strong tendency for tertiary radical formation, we believe this is a second-order effect, and to a first approximation can be neglected.

## Conclusions

We have observed unsaturated chain ends, created by high-temperature extrusion, in ethylene–propylene copolymers. Vinyl, vinylene, and vinylidene chain ends were observed and quantified by  $^1\text{H}$  NMR. We have compiled all possible types of olefin chain ends that could form from chain scission of ethylene–propylene copolymers and calculated their  $^{13}\text{C}$  chemical shifts. These results were then used to assign the olefin region of the  $^{13}\text{C}$  NMR spectrum of the sheared polymer.

The mechanism of polymer shearing appears to be hydrogen abstraction followed by disproportionation to form olefins. The methine proton is preferentially abstracted by a ratio of more than 6:1, relative to a proton on a secondary carbon. Furthermore, following C–H scission, there is a preference toward main chain scission at the  $\beta$ -position relative to the radical, by over 2:1.

In conclusion, we have characterized an important terminal functionalization of the polymer chains occurring during high-temperature extrusion. We feel the results reported in this paper will lead to an increased understanding about the chemistry involved in a process in commercial use worldwide.

**Acknowledgment.** We thank Mr. Gary Spedale, Mr. Walter Van Osdell, and Mr. Darren Cothren for the preparation of the highly sheared polymers used in this study, Mr. Roland Spano and Dr. Suzanne Sellers for SEC measurements, and Dr. Mary Schexnayder for helpful discussions on free radical chemistry. We would also like to thank Dr. Harold Young and Dr. Jeffrey Crow for helpful discussions and advice throughout the course of this project.

## References and Notes

- (1) Barakos, G.; Mitsoulis, E.; Tzoganakis, C.; Kajiwar, T. *J. Appl. Polym. Sci.* **1996**, *59*, 543.
- (2) Krell, M. J.; Brandolin, A.; Valles, E. M. *Polym. React. Eng.* **1994**, *2*, 389.
- (3) Tzoganakis, C. *Can. J. Chem. Eng.* **1994**, *72*, 749.
- (4) Lederer, K.; Beytollahiamtmann, I.; Billiani, J. *J. Appl. Polym. Sci.* **1994**, *54*, 47.
- (5) Tollefon, N. M. *J. Appl. Polym. Sci.* **1994**, *52*, 905.
- (6) Ryu, S. H.; Gogos, C. G.; Xanthas, M. *Polymer* **1991**, *32*, 2449.
- (7) Pospisil, L.; Rybníkar, F. *Polymer* **1990**, *31*, 476.
- (8) Rideal, G. R.; Padget, J. C. *J. Polym. Sci.* **1976**, *57*, 1.
- (9) Vangisbergen, J. G. M.; Meijer, H. E. H.; Lemstra, P. J. *Polymer* **1989**, *30*, 2153.
- (10) O'Donnell, J.; Whittaker, A. *Polymer* **1992**, *33*, 62.
- (11) Sohma, J. *Prog. Polym. Sci.* **1989**, *14*, 451.
- (12) Sohma, J.; Sakaguchi, M. *Adv. Polym. Sci.* **1976**, *20*, 109.
- (13) Andrew, E. H.; Reed, P. E. *Adv. Polym. Sci.* **1978**, *27*, 1.
- (14) Butyagin, P.; Abagian, B. *Biophysics* **1964**, *9*, 161.
- (15) Sakaguchi, M.; Sohma, J. *J. Polym. Sci.* **1975**, *13*, 1233.
- (16) Lazar, M.; Szocs, F. *J. Polym. Sci. C* **1967**, *16*, 461.
- (17) Backman, D. K.; Devries, K. L. *J. Polym. Sci., Polym. Chem. Ed.* **1969**, *7*, 2125.
- (18) Verima, G. S. P.; Peterlin, A. *Kolloid Z. Polym.* **1970**, *236*, 111.

- (19) Nagamura, T.; Takayanagi, M. *J. Polym. Sci. Phys.* **1974**, *12*, 2019.
- (20) Natarjan R.; Reed, P. E. *J. Polym. Sci., Polym. Phys. Ed.* **1972**, *10*, 585.
- (21) Kawashima, T.; Nakamura, N.; Shimada, S.; Kashhiwabara, H.; Sohma, J. *Rep. Prog. Polym. Phys. Jpn.* **1969**, *12*, 469.
- (22) Tabata, M.; Miyazawa, T.; Kobayashi, O.; Sohma, J. *Chem. Phys. Lett.* **1980**, *73*, 178.
- (23) Tabata, M.; Hosokawa, Y.; Watanabe, O.; Sohma J., *Polym. J.* **1986**, *18*, 699.
- (24) Sohma, J. *Colloid Polym. Sci.* **1992**, *270*, 1060.
- (25) Oakes, W. G.; Richards, R. B. *J. Chem. Soc.* **1949**, 2929.
- (26) Zhurkov, S. N.; Novak, I. I.; Vettegren, V. I. *Dokl. Akad. Nauk SSSR* **1964**, *157*, 1431.
- (27) Zambelli, A.; Locatelli, P.; Sacchi, M. C.; Rigamonti, E. *Macromolecules* **1980**, *13*, 798.
- (28) Zambelli, A.; Sacchi, M. C.; Locatelli, P.; Zannoni, G. *Macromolecules* **1982**, *15*, 211.
- (29) Rossi, A.; Zhang, J.; Odian, G. *Macromolecules* **1996**, *29*, 2331.
- (30) Cheng, H. N. *Macromol. Symp.* **1994**, *86*, 77.
- (31) Cheng, H. N.; Smith, D. A. *Macromolecules* **1986**, *19*, 2065.
- (32) Bueche, F. *J. Appl. Polym. Sci.* **1960**, *9*, 101.
- (33) Veselovskaya, E. V.; Kreitser, T. V.; Severova, N. N.; Goldenberg, A. L.; L'vovskii, V. E.; Grigoriev, V. A. *Int. Polym. Sci. Technol.* **1979**, *6*, 5.
- (34) Tsutsui, T.; Mizuno, A.; Kashiwa, N. *Polymer* **1989**, *30*, 428.
- (35) Couperous, P. A.; Clague, A. D. H.; van Dongen, J. P. C. M. *Org. Magn. Reson.* **1976**, *8*, 426.
- (36) From a spectrum of 2-methyl-1-octene,<sup>35</sup> however, Cheng<sup>31</sup> observes the reported shifts in low molecular weight EP.
- (37) 4-Methyl-1-hexene.<sup>35</sup>
- (38) 5-Methyl-1-hexene.<sup>35</sup>
- (39) Calculated in the present work.
- (40) 2, 4-Dimethyl-1-pentene.<sup>35</sup>
- (41) 2-Decene in: de Haan, J. W.; van de Ven, L. J. M. *Org. Magn. Reson.* **1973**, *5*, 147.
- (42) 2-Methyl-2-heptene.<sup>35</sup>
- (43) 3-Methyl-2-hexene.<sup>35</sup>
- (44) 4-Methyl-2-hexene.<sup>35</sup>
- (45) 5-Methyl-2-hexene.<sup>35</sup>
- (46) 2,4-Dimethyl-2-pentene.<sup>35</sup>
- (47) 2,5-Dimethyl-2-hexene.<sup>35</sup>
- (48) 2,6-Dimethyl-2-octene.<sup>35</sup>
- (49) Zhurkov, S. N.; Zakrevskiy, V. A.; Korsukov, V. E.; Kuksenko, V. S. *J. Polym. Sci., Polym. Phys. Ed.* **1972**, *10*, 1509.
- (50) Zakrevskiy, V. A.; Korsukov, V. E. *Vysokmol. Soedin A* **1972**, *14*, 955.
- (51) Carman, C. J.; Harrington, R. A.; Wilkes, C. E. *Macromolecules* **1977**, *10*, 536.
- (52) Randall, J. C. *Macromolecules* **1978**, *11*, 33.
- (53) Cheng, H. N. *Macromolecules* **1984**, *17*, 1950.
- (54) DiMartino, S.; Kelchtermans, M. *J. Appl. Polym. Sci.* **1995**, *56*, 1781.
- (55) Kakugo, M.; Naito, Y.; Mizunuma, K.; Miyatake, T. *Macromolecules* **1982**, *15*, 1150.
- (56) Johnston, J. E.; Bloch, R.; Ver Strate, G. W.; Song, W. R. U.S. Patent number 4,507,515, 1985.
- (57) Kresge, E. N.; Cozewith, C.; Ver Strate, G. "Long Chain Branching and Gel in EPDM", Presentation at Rubber Division ACS symposium, Indianapolis, IN 1984.

MA961099Q